Proceedings of Inverse Problems in Engineering : Theory and Practice
3rd Int. Conference on Inverse Problems in Engineering
June 13-18, 1999, Port Ludlow, WA, USA

ID02

ON THE IDENTIFICATION OF NONLINEAR CONSTITUTIVE LAWS FROM INDENTATION TESTS

Nicolas Tardieu , Andrei Constantinescu
Laboratoire de Mécanique des Solides
CNRS UMR 7649
Ecole Polytechnique
91128 Palaiseau Cedex
FRANCE
Email: tardieu;constant@lms.polytechnique.fr

ABSTRACT

This paper addresses the identification of the parameters of a nonlinear constitutive law from indentation tests. The case of a standard generalized material without work hardening is extensively treated using the adjoint state method. This provides a general framework to perform optimization involving contact conditions and nonlinear material behaviour. A numerical identification is presented and demonstrates the accuracy and the robustness of the method.

INTRODUCTION

The indentation test consists in pressing a punch on a material sample. It was initialy used to evaluate the hardness of metals and is now being considered as an efficient non destructive method for determining material mechanical characteristics (Taljat et al.,1998).

The constitutive law is to be identified from the knowledge of the indentation curve, representing the load applied on the punch versus the penetration depth. The mechanical interpretation of the indentation curve is not as straightforward as for the classical traction curve. This implies that the use of the indentation test for material characterization depends on the reliability of the subsequent identification procedure. Most identification strategies are based on semi-empirical formulas dedicated to a given constitutive behaviour : elasticity, perfect plasticity (Johnson,1985), power laws (Jayaraman et al., 1998), ... Only a few studies present this problem from a general point of view, i.e. defining the identification as the minimization of a cost functional (Bui, 1994). The identification methods are generally based on simple *trial & error* techniques (Hasanov & Seyidmamedov , 1995). This is partly due to the mathematical complexity of the contact description, appearing independently of the constitutive behaviour of the material.

A first attempt to solve the problem from a general point of view has been presented in the case of linear elasticity (Constantinescu & Tardieu, 1995). The contact conditions having been regularized by penalization, the problem was therefore described by variational equalities, instead of variational inequalities. This enables the application of classical optimal control (Lions,1968) techniques, in particular the adjoint state method. The identification problem has been solved afterwards by the minimization of a cost functional using a gradient descent method.

The goal of this paper is to extend this method to the identification of the parameters of a standard generalized constitutive law without work hardening. The method presented in this paper is not based on the regularization of the contact conditions as in (Constantinescu & Tardieu, 1995), instead Lagrange multipliers are used. The gradient of the cost functional is computed from the solution of a direct and an adjoint problem. The accuracy and robustness of the method are illustrated through a numerical example for a Maxwell viscoelastic constitutive law.

Copyright © 1999 by ASME

THE DIRECT PROBLEM (P)

Let us consider an axisymmetric body, with its section occupying in its reference configuration an open subset $\Omega \subset \mathbb{R}^2$ with smooth boundary Γ (see Figure 1). The boundary is partitioned in three parts $\Gamma = \Gamma_D \cup \Gamma_F \cup \Gamma_C$: the part Γ_D where displacements are imposed, the free surface Γ_F, and the surface Γ_C where contact might occur. $\boldsymbol{n}$ and $\boldsymbol{t}$ denote the normal and tangent vector to the boundary Γ.

The axisymmetric hypothesis is taken in order to simplify the presentation and the computational burden and does not restrict the generality of the method.

The problem will be treated within the theory of small strains and rotations. The validity of this hypothesis will be discussed later. Let us denote respectively by $\boldsymbol{u}$, $\boldsymbol{\varepsilon}$ and $\boldsymbol{\sigma}$ the vector field of displacements and the tensor fields of small strains and stresses.

The problem considered in the sequel is the indentation of the body Ω by a rigid punch whose profile is characterized by the gap g. The contact is considered without friction.

An indentation experiment is driven either by the vertical displacement U or by the force F applied to the punch. The force F can be expressed as integral of the contact pressure:

$$F = \int_{\Gamma_C} \boldsymbol{n} \cdot \boldsymbol{\sigma} \cdot \boldsymbol{n} \, d\Gamma$$

An experiment provides an indentation curve (see Figure 3), representing a displacement-force history (U^{exp}, F^{exp}) over a given time interval $[0, T]$.

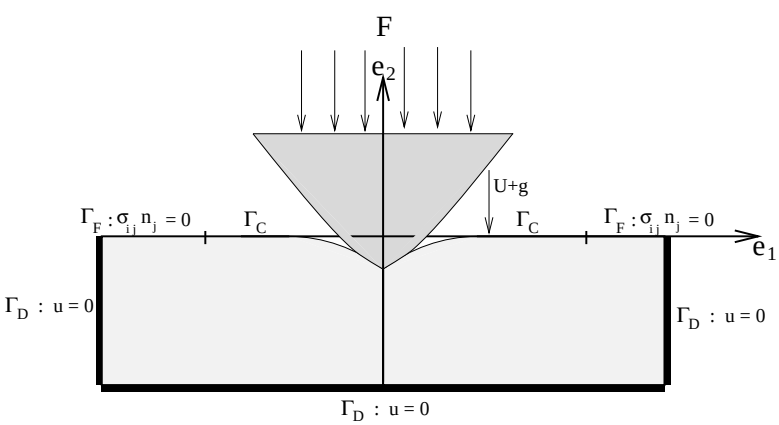

Figure 1. THE DIRECT PROBLEM

In this work, we have always considered the problem as driven by the punch displacement. The governing equations can be written using:

- a *time-continous formulation*, where the intervening quantities are the field rates, or
- a *time-dicretized formulation*, where the intervening quantities are small increments of the fields between two time steps.

Describing contact conditions using the field rates is a complicated task requiring care in the choice of the functional spaces of the mathematical formulations (Kikuchi & Oden,1988). Therefore the time dicretized expression, which permits to avoid some of these difficulties, will be used in this paper.

Constitutive law

A standard generalized material without work hardening (Halphen & Nguyen,1975) is considered here. This constitutive behaviour is completely determined by the elasticity tensor $\boldsymbol{S}(\boldsymbol{c})$ and by the pseudo-potential of dissipation $\Phi = \Phi(\boldsymbol{\sigma}, \boldsymbol{c})$. The latter is supposed to be twice differentiable with respect to $\boldsymbol{\sigma}$. $\boldsymbol{c}$ is the vector of the material parameters characterizing the material behaviour (Young's modulus, elasticity limit, ...).

Time-continuous formulation

In a time continuous description, the constitutive law is expressed by the classical set of equations:

$$\boldsymbol{\varepsilon}(\dot{\boldsymbol{u}}) = \boldsymbol{S}(\boldsymbol{c}) : \dot{\boldsymbol{\sigma}} + \dot{\boldsymbol{\varepsilon}}^p \tag{1}$$

$$\dot{\boldsymbol{\varepsilon}}^p = \frac{\partial \Phi(\boldsymbol{\sigma}, \boldsymbol{c})}{\partial \boldsymbol{\sigma}} \tag{2}$$

where the dot $(\dot{\ })$ denotes the time derivative and $\boldsymbol{\varepsilon}^p$ is the viscoplastic strain.

Time-discretized formulation

In a time discretization, the previous equations are expressed as :

$$\boldsymbol{\varepsilon}(\Delta \boldsymbol{u}_i) = \boldsymbol{S}(\boldsymbol{c}) : \Delta \boldsymbol{\sigma}_i + \Delta \boldsymbol{\varepsilon}_i^p \tag{3}$$

$$\Delta \boldsymbol{\varepsilon}_i^p = \frac{\partial \Phi(\boldsymbol{\sigma}_i, \boldsymbol{c})}{\partial \boldsymbol{\sigma}} \Delta t \tag{4}$$

Example

The following classical constitutive laws can be expressed under this formalism :

- The Maxwell viscoelastic material : the pseudo-potential Φ is given by $\Phi(\boldsymbol{\sigma}_i, \boldsymbol{c}) = \frac{1}{2} \boldsymbol{\sigma}_i : \boldsymbol{M}(\boldsymbol{c}) : \boldsymbol{\sigma}_i$ where $\boldsymbol{M}(\boldsymbol{c})$ is a forth order tensor and $\boldsymbol{c} = \{E, \eta\}$. The inelastic strain increment is determined by : $\Delta \boldsymbol{\varepsilon}_i^p = \boldsymbol{M}(\boldsymbol{c}) : \boldsymbol{\sigma}_i \Delta t$.

Copyright © 1999 by ASME

• The Norton-Hoff viscoplastic material : the pseudo potential Φ is given by $\Phi(\boldsymbol{\sigma}_i,\boldsymbol{c}) = \dfrac{1}{m+1}\langle(\boldsymbol{\sigma}_i)_{eq} - \sigma^Y\rangle_+^{m+1}$ where σ^Y is the elasticity limit, $\langle\cdot\rangle_+$ is the positive part operator, $(\cdot)_{eq}$ is the equivalent Mises stress and $\boldsymbol{c} = \{E,\sigma^Y,m\}$. The plastic strain increment is determined by : $\Delta\boldsymbol{\varepsilon}_i^p = \dfrac{3}{2}\langle(\boldsymbol{\sigma}_i)_{eq} - \sigma^Y\rangle_+^m \dfrac{\tilde{\boldsymbol{\sigma}}_i}{(\boldsymbol{\sigma_i})_{eq}}\Delta t$; $\tilde{\boldsymbol{\sigma}}_i$ is the deviator of $\boldsymbol{\sigma}_i$.

Equations of the direct problem (P)

The governing equations of the direct problem consist of the equilibrium and constitutive equations, the boundary and contact conditions and a set of initial values. The contact conditions on Γ_C will be expressed using the Lagrange multipliers $p_i \in N$, where $N = \{q \in (H^{1/2}(\Gamma_C))' \quad | \quad q \leq 0\}$ is a closed convex set and $(H^{1/2}(\Gamma_C))'$ denotes the dual of $H^{1/2}(\Gamma_C)$ (Kikuchi & Oden,1988). The Lagrange multipliers p_i will show up to be the pressure distribution under the punch. g_i denote the gap at time t_i i.e. $g_i = u_i^n - g - U_i$.

Equilibrium and constitutive equation in Ω

$$div(\Delta\boldsymbol{\sigma}_i) = 0 \tag{5}$$

$$\boldsymbol{\varepsilon}(\Delta\boldsymbol{u}_i) = \boldsymbol{S}(\boldsymbol{c}) : \Delta\boldsymbol{\sigma}_i + \frac{\partial\Phi(\boldsymbol{\sigma}_i,\boldsymbol{c})}{\partial\boldsymbol{\sigma}}\Delta t \tag{6}$$

Boundary conditions

$$\Delta\boldsymbol{\sigma}_i \cdot \boldsymbol{n} = 0 \ \text{ on } \ \Gamma_F \tag{7}$$

$$\Delta\boldsymbol{u}_i = 0 \ \text{ on } \ \Gamma_D \tag{8}$$

Contact conditions

$$(\Delta u_i^n - g_i - \Delta U_i)(q - p_{i+1}) \geq 0 \ \ \forall q \in N \tag{9}$$

$$\Delta\sigma_i^{nn} = \Delta\boldsymbol{\sigma}_i \cdot \boldsymbol{n} \cdot \boldsymbol{n} = \Delta p_i \tag{10}$$

$$\Delta\sigma_i^{nt} = (\Delta\boldsymbol{\sigma}_i \cdot \boldsymbol{n} - \Delta\sigma_i^{nn} \cdot \boldsymbol{n}) \cdot \boldsymbol{t} = 0 \tag{11}$$

Initial conditions

$$\boldsymbol{\sigma}_0 = 0 \ \text{ in } \ \Omega \tag{12}$$

$$\boldsymbol{u}_0 = 0 \ \text{ on } \ \Omega \tag{13}$$

$$\boldsymbol{\varepsilon}_0^p \cdot \boldsymbol{n} = 0 \ \text{ on } \ \Omega \tag{14}$$

$$\tag{15}$$

THE INVERSE PROBLEM (P^{-1})

In the present inverse problem, one wants to identify the parameters of the material behaviour $\boldsymbol{c}$ from the knowledge of the indentation curve (U^{exp}, F^{exp}). $\boldsymbol{c}$ is supposed to belong to a closed convex subset Q of $\mathbb{R}^n$ $(n \geq 2)$.

This inverse problem can be expressed as a minimization problem of a well-chosen cost functional. Since the direct problem is driven by the imposed displacement of the punch U, it is natural to express the cost functional as a function of the resultant force F. A possible formulation of the inverse problem (P^{-1}) is thus :

Find $\boldsymbol{c} \in Q$ *minimizing*

$$\begin{aligned} J(\boldsymbol{c}) &= \frac{1}{2}\sum_{i=0}^{I}(F_i^{comp}(\boldsymbol{c}) - F_i^{exp})^2 \\ &= \frac{1}{2}\sum_{i=0}^{I}(\int_{\Gamma_C} p_i(\boldsymbol{c})d\Gamma - F_i^{exp})^2 \end{aligned} \tag{16}$$

where, F^{comp} *is the computed resultant force from the direct problem driven by* U^{exp}.

One can remark that the cost functional J depends implicitly on the material parameters $\boldsymbol{c}$ through the pressure distribution p. The resolution of the direct problem (P) permits the determination of the Lagrange multiplier p_i and then the calculation of F_i^{comp}. In consequence, this minimization problem can be considered as a constrained one, the constraint being the resolution of (P).

To our knowledge, no existence or uniqueness results are available for this problem. This might be a consequence of the difficulties implied by the strong nonlinearity imposed by the nonlinear constitutive law and the presence of contact. Moreover, no convexity properties are known about this functional. After drawing some numerical examples for a series of problems, some uniqueness and stability conjectures will be made.

Resolution

Finding the minimum of a constrained minimization problem is equivalent, under some regularity conditions, to finding the saddle point of a Lagrangian functional L. Generally, the Lagrangian L is introduced as a sum of the cost functional and a variational formulation of the direct problem (P).

Let us introduce, for each variable of the direct problem, an adjoint variable, denoted by a $\star$ superscript. These adjoint variables are the Lagrange multipliers of the equations of the direct problem, acting as constraints.

According to the optimal control theory, all direct and adjoint variables will be considered mutually independent. The relationships between them will be recovered from the stationarity conditions of the Lagrangian L, characterizing the saddle point.

Copyright © 1999 by ASME

The Lagrangian functional has the following form :

$$L(\boldsymbol{u},\boldsymbol{\sigma},p,\boldsymbol{u}^\star,\boldsymbol{\sigma}^\star,p^\star,\boldsymbol{c}) = \sum_{i=0}^{I} L_i(\boldsymbol{u}_i,\boldsymbol{\sigma}_i,p_i,\boldsymbol{u}_i^\star,\boldsymbol{\sigma}_i^\star,p_i^\star,\boldsymbol{c})$$

where each term L_i is obtained as the sum of the cost functional at time t_i and the direct time-discretized equations, multiplied by the corresponding adjoint variables.

$$\begin{aligned}
L_i(\boldsymbol{u}_i,\,\boldsymbol{\sigma}_i\,,p_i,\boldsymbol{u}_i^\star,\boldsymbol{\sigma}_i^\star,p_i^\star) &= \frac{1}{2}\Big(\int_{\Gamma_C} p_i d\Gamma - F_i^{exp}\Big)^2 \\
&+ \int_\Omega div(\Delta\boldsymbol{\sigma}_i)\cdot\boldsymbol{u}_i^\star d\Omega - \int_{\Gamma_F} \Delta\boldsymbol{\sigma}_i\cdot\boldsymbol{n}\cdot\boldsymbol{u}_i^\star d\Gamma \\
&+ \int_{\Gamma_D} \Delta\boldsymbol{u}_i\cdot\boldsymbol{\sigma}_i^\star\cdot\boldsymbol{n} d\Gamma + \int_{\Gamma_C} (\Delta u_i^n - \Delta U_i - g_i)\cdot p_i^\star d\Gamma \\
&- \int_\Omega \Big(\boldsymbol{\varepsilon}(\Delta\boldsymbol{u}_i) - \boldsymbol{S}(\boldsymbol{c}) : \Delta\boldsymbol{\sigma}_i - \frac{\partial\Phi(\boldsymbol{\sigma}_i,\boldsymbol{c})}{\partial\boldsymbol{\sigma}}\Delta t\Big) : \boldsymbol{\sigma}_i^\star d\Omega \\
&- \int_{\Gamma_C} (\Delta p_i - \Delta\boldsymbol{\sigma}_i^{nn})\cdot u_i^{n\star} d\Gamma - \int_{\Gamma_C} \Delta\sigma_i^{nt}\cdot u_i^{t\star} d\Gamma
\end{aligned}$$

and

- $\boldsymbol{u}_i,\boldsymbol{u}_i^\star \in (H^1(\Omega))^2$
- $\boldsymbol{\sigma}_i,\boldsymbol{\sigma}_i^\star \in (L^2(\Omega))^4$
- $p_i,p_i^\star \in N_i = \{q \in (H^{1/2})'(\Gamma_C) \quad | \quad q = 0 \text{ on } \Gamma_{C_i}\}$, where Γ_{C_i} is the effective contact surface at time t_i.

The complex form of this Lagrangian does not permit to draw any conclusions with regard to the existence and uniqueness of its saddle point. Nevertheless, necessary conditions of stationarity can formally be written in order to characterize this possible saddle point ; they read :.

$$\sum_{i=0}^{I}\left\langle \frac{\partial L_i}{\partial\boldsymbol{u}}, d\boldsymbol{w}_i\right\rangle = 0 \;\; \forall d\boldsymbol{w}_i \in (H^1(\Omega))^2 \tag{17}$$

$$\sum_{i=0}^{I}\left\langle \frac{\partial L_i}{\partial\boldsymbol{\sigma}}, d\boldsymbol{\tau}_i\right\rangle = 0 \;\; \forall d\boldsymbol{\tau}_i \in (L^2(\Omega))^4 \tag{18}$$

$$\sum_{i=0}^{I}\left\langle \frac{\partial L_i}{\partial p}, dq_i\right\rangle = 0 \;\; \forall dq_i \in N_i \tag{19}$$

$$\sum_{i=0}^{I}\left\langle \frac{\partial L_i}{\partial\boldsymbol{u}^\star}, d\boldsymbol{w}_i\right\rangle = 0 \;\; \forall d\boldsymbol{w}_i \in (H^1(\Omega))^2 \tag{20}$$

$$\sum_{i=0}^{I}\left\langle \frac{\partial L_i}{\partial\boldsymbol{\sigma}^\star}, d\boldsymbol{\tau}_i\right\rangle = 0 \;\; \forall d\boldsymbol{\tau}_i \in (L^2(\Omega))^4 \tag{21}$$

$$\sum_{i=0}^{I}\left\langle \frac{\partial L_i}{\partial p^\star}, dq_i\right\rangle = 0 \;\; \forall dq_i \in N_i \tag{22}$$

$$\sum_{i=0}^{I}\left\langle \frac{\partial L_i}{\partial\boldsymbol{c}}, \boldsymbol{d}-\boldsymbol{c}\right\rangle \geq 0 \;\; \forall\boldsymbol{d} \in Q \tag{23}$$

where $\langle\,\cdot\,,\;\cdot\,\rangle$ represents in each equation the duality pairing for the corresponding functional spaces.

Calculating the derivatives with respect to the adjoint variables (equations (20), (21) and (22)) leads to the set of equations :

$$div(\Delta\boldsymbol{\sigma}_i) = 0 \;\text{ in }\; \Omega \tag{24}$$

$$\boldsymbol{\varepsilon}(\Delta\boldsymbol{u}_i) - \boldsymbol{S}(\boldsymbol{c}) : \Delta\boldsymbol{\sigma}_i - \frac{\partial\Phi(\boldsymbol{\sigma}_i,\boldsymbol{c})}{\partial\boldsymbol{\sigma}}\Delta t = 0 \;\text{ in }\; \Omega \tag{25}$$

$$\Delta\boldsymbol{\sigma}_i\cdot\boldsymbol{n} = 0 \;\text{ on }\; \Gamma_F \tag{26}$$

$$\Delta\boldsymbol{u}_i = 0 \;\text{ on }\; \Gamma_D \tag{27}$$

$$\left.\begin{aligned}
&\Delta u_i^n - g_i - \Delta U_i = 0 \\
&\Delta\boldsymbol{\sigma}_i\cdot\boldsymbol{n}\cdot\boldsymbol{n} = \Delta p_i \\
&\Delta\sigma_i^{nt} = 0
\end{aligned}\right\} \text{ on } \Gamma_{C_i} \tag{28}$$

The previous calculation leads in classical Lagrangian theory to the equations of the direct problem. In the present case, opposite to the classical frame, the equations do not represent exactly the direct problem. However, if $(\boldsymbol{u},\boldsymbol{\sigma},p)$ are the solutions to (P), they obviously verify the above relations.

The differentiation of L with respect to the direct variables (equations (17), (18) and (19)) and a series of calculations : spatial integration by parts and use of the relation $f_i\cdot\Delta g_i = f_{i+1}\cdot g_{i+1} - f_i\cdot g_i - \Delta f_i\cdot g_i$, gives the following set of equations :

$$div(\Delta\boldsymbol{\sigma}_i) = 0 \;\text{ in }\; \Omega \tag{29}$$

$$\boldsymbol{\varepsilon}(\Delta\boldsymbol{u}_i^\star) = \boldsymbol{S}(\boldsymbol{c}) \;:\Delta\boldsymbol{\sigma}_i^\star - \frac{\partial^2\Phi(\boldsymbol{\sigma}_i,\boldsymbol{c})}{\partial\boldsymbol{\sigma}^2}\Delta t : \boldsymbol{\sigma}_i^\star \;\text{ in }\; \Omega \tag{30}$$

$$\Delta\boldsymbol{\sigma}_i^\star\cdot\boldsymbol{n} = 0 \;\text{ on }\; \Gamma_F \tag{31}$$

$$\Delta\boldsymbol{u}_i^\star = 0 \;\text{ on }\; \Gamma_D \tag{32}$$

$$\left.\begin{aligned}
&\Delta u_i^{n\star} = (F_i^{calc}(\boldsymbol{c}) - F_i^{exp}) \\
&\Delta\sigma_i^{nn\star} = \Delta p_i^\star \\
&\Delta\sigma_i^{nt\star} = 0
\end{aligned}\right\} \text{ on } \Gamma_{C_i} \tag{33}$$

and the following final conditions at time T :

Copyright © 1999 by ASME

$$div(\boldsymbol{\sigma}_I^\star) = 0 \ \text{ in } \ \Omega \tag{34}$$

$$\boldsymbol{\varepsilon}(\Delta \boldsymbol{u}_I^\star) = \boldsymbol{S}(\boldsymbol{c}) : \Delta \boldsymbol{\sigma}_I^\star \ \text{ in } \ \Omega \tag{35}$$

$$\boldsymbol{u}_I^\star = 0 \ \text{ on } \ \Gamma_D \tag{36}$$

$$\boldsymbol{\sigma}_I^\star \cdot \boldsymbol{n} = 0 \ \text{ on } \ \Gamma_F \tag{37}$$

$$\left.\begin{array}{l} u_i^{n\star} = 0 \\ p_I^\star = \sigma_I^{nn\star} \end{array}\right\} \ \text{ on } \ \Gamma_C \tag{38}$$

The equations (29)-(33) and the final conditions (34)-(38) define a well-posed incremental problem with Dirichlet conditions on a part of the boundary and will be called the adjoint problem $(P^\star)$.

As a consequence of the preceding calculations the following result can be stated :

Stationarity Result:

If $(\boldsymbol{u}, \boldsymbol{\sigma}, p)$ and $(\boldsymbol{u}^\star, \boldsymbol{\sigma}^\star, p^\star)$ are respectively the solutions to the incremental direct and adjoint problem (P) and $(P^\star)$, then the conditions (17), (18), (19), (20), (21) and (22) of stationarity of the Lagrangian L are verified.

Moreover, if $(\boldsymbol{u}, \boldsymbol{\sigma}, p)$ are the solutions to (P), one can notice that the Lagrangian L is reduced to the cost functional J. Together with the expression of stationarity conditions (23) this implies that :

Gradient Computation:

If $(\boldsymbol{u}, \boldsymbol{\sigma}, p)$ and $(\boldsymbol{u}^\star, \boldsymbol{\sigma}^\star, p^\star)$ are respectively the solutions to the incremental direct problem (P) and to the incremental adjoint problem $(P^\star)$, then the gradient of the cost functional J is given by :

$$\nabla_{\boldsymbol{c}} J = \sum_{i=0}^{I} \left(\int_\Omega \Delta \boldsymbol{\sigma}_i : \frac{\partial \boldsymbol{S}}{\partial \boldsymbol{c}} : \boldsymbol{\sigma}_i^\star + \frac{\partial^2 \Phi}{\partial \boldsymbol{\sigma} \partial \boldsymbol{c}} \Delta t : \boldsymbol{\sigma}_i^\star \, d\Omega \right) \tag{39}$$

Some remarks about the preceding results are as follows :

- The adjoint problem is a time-dependent system of partial differential equations on $[0, T]$. We dispose of a final condition instead of the more usual initial condition. We shall therefore speak of a reversed-time problem. The final condition is given by a well-posed elasticity problem.
- The adjoint problem is *not* a contact problem. Its loading is a Dirichlet conditions (imposed displacement) on Γ_{C_i}, the effective contact surface of the direct problem.
- The adjoint constitutive law is viscoelastic considered in the reversed time $i' \leftarrow I - i$:

$$\boldsymbol{\varepsilon}(\Delta \boldsymbol{u}_{i'}^\star) = \boldsymbol{S}(\boldsymbol{c}) : \Delta \boldsymbol{\sigma}_{i'}^\star + \boldsymbol{R} : \boldsymbol{\sigma}_{i'}^\star \, \Delta t$$

where $\boldsymbol{R}$ is the fourth order tensor :

$$\boldsymbol{R} = \frac{\partial^2 \Phi(\boldsymbol{\sigma}_{i'}, \boldsymbol{c})}{\partial \boldsymbol{\sigma}_{i'}^2} \ .$$

This is why the pseudo-potential Φ has to be twice differentiable (For example, in the Norton-Hoff constitutive law, $m > 2$ is needed). The parameters of this constitutive law depend on the parameters of the direct constitutive law, and also on the solution of the direct problem. From a numerical point of view, this conducts to a linear problem at each time step and therefore a rapid integration.

- The solution to the adjoint problem is implicitly dependent on the solution of the direct problem.
- This method allows the computation of the gradient of the cost functional J using the solutions to the direct and adjoint problems, independently of the number of parameters involved. A rapid evaluation of the computational burden shows that a gradient calculation takes ≈ 1.2 the time for solving the direct problem due to the simplicity of the adjoint behaviour and the elimination of the contact conditions. This is extremely interesting for problems with a large number of parameters. However, the discrete convolution nature of (39) and the time-reversed character of the adjoint problem require the storage of the complete histories of all direct variables.

NUMERICAL EXAMPLE

In order to illustrate the presented method, let us consider the identification of the parameters of a Maxwell viscoelastic material :

$$\boldsymbol{\varepsilon}(\Delta \boldsymbol{u}_i) = \boldsymbol{S} : \Delta \boldsymbol{\sigma}_i + \Delta \boldsymbol{\varepsilon}_i^p \quad \text{where} \quad \Delta \boldsymbol{\varepsilon}_i^p = \boldsymbol{M} : \boldsymbol{\sigma}_i \Delta t \tag{40}$$

$$S_{ijkl} = \frac{1}{E}((1+\nu)\delta_{ik}\delta_{jl} - \nu\delta_{kl}\delta_{ij}) \tag{41}$$

$$M_{ijkl} = \frac{1}{\eta}(\delta_{ik}\delta_{jl} - \frac{1}{3}\delta_{kl}\delta_{ij}) \tag{42}$$

where E, ν, η denote respectively the Young modulus, the Poisson coefficient and the viscosity.

As explained before, this constitutive law enters the formalism of the standard generalized materials without work-hardening.

The identification problem consists in determining E and η from a indentation curve (U^{exp}, F^{exp}). In this work the indentation curve is obtained from numerical experiments as explained in the sequel.

Copyright © 1999 by ASME

Direct calculations

The experiment simulations have been realized through finite elements computations using the CASTEM2000 finite element code. The body Ω is a cylinder with radius 10 mm and height 10 mm and the punch is a rigid cone with a 68° half angle at the apex. The mesh of the body was composed of 20×20 quadratic elements.

The indentation process is displacement-controlled and consists of loading, maintain and unloading parts (Figure 2). A typical indentation curve is represented on Figure 3.

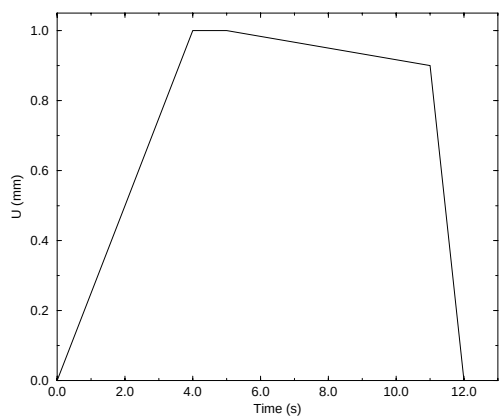

Figure 2. LOADING HISTORY OF THE INDENTOR

The hypothesis of small strains and rotations has been the key assumption in the development of the calculations of the adjoint state method. It was therefore important to validate this assumption. A series of direct computations has been done in three different cases : small strains and rotations, large strains and large strains and rotations, with $E = 2 \times 10^4$ MPa and $\eta = 3 \times 10^4$ MPa/s. The results show a good agreement of the indentation curves (see Figure 3). It is important to remark that the small difference is due in part to the simple constitutive law assumed. This hypothesis should be checked before applying this method for other constitutive laws.

Identification procedure

The identification procedure presented next is based on minimization of the cost functional J given in (16) using a gradient descent method. The "experimental" curve was simulated by finite element calculations as stated in the previous section with $E = 2 \times 10^4$ MPa , $\nu = 0.3$, $\eta = 3 \times 10^4$ MPa/s.

The gradient has been computed using the adjoint state method with the expression (39) after solving the direct problem (P) and the adjoint problem $(P^\star)$. In the case of the Maxwell material behaviour, the adjoint behaviour is also a Maxwell law. This is due to the quadratic viscoelastic potential Φ, which is self-adjoint.

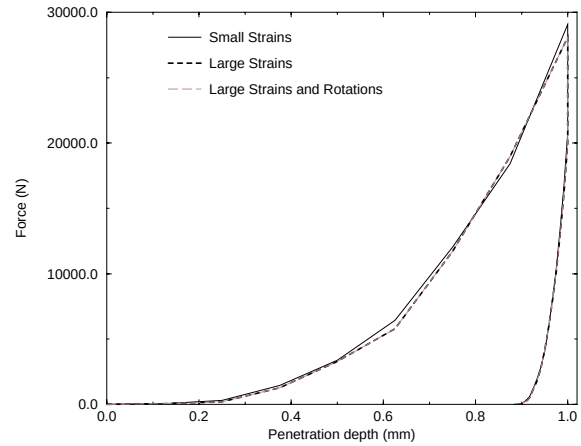

Figure 3. INDENTATION CURVES FOR SMALL AND LARGE STRAINS HYPOTHESIS

The numerical gradient computation by the adjoint method has been compared with a computation by finite differences. The results for several points and directions showed less than 10% difference between the two methods.

The minimization algorithm was the quasi-Newton BFGS algorithm with a line search obeying the Armijo selection rule (Gill, Murray, Wright,1981).

The shape of the cost functional has been plotted in Figure 4 from a series of direct computations. We notice a smooth flat valley which should not pose special difficulties to the identification.

Identification using exact "measurements"

A first series of identifications have been performed with exact simulated measurements. The results for different initial points are presented in Table 1. The starting values of $(E, \eta)$for the algorithm have been at maximum 5 times smaller or 3 times larger than the real values. In all cases the final value was less than 0.02% from the value to be identified, after about 15 iterations. Some typical evolution path of the algorithm on the isovalues of the cost functional are plotted in Figure 5.

Figure 6 shows the real indentation curve in comparison to the initial and converged indentation curve. In terms of cost functional the algorithm brought its value from $\approx 10^8$ to $\approx 10^1$.

Identification using "measurements" with random error

In order to check the robustness of the identification procedure the simulated measurements have been perturbed by a 10% random noise. The results of several identifications using perturbed measurement data are presented in Table 2. The first pair and the last pair of data are results coming from identification

Copyright © 1999 by ASME

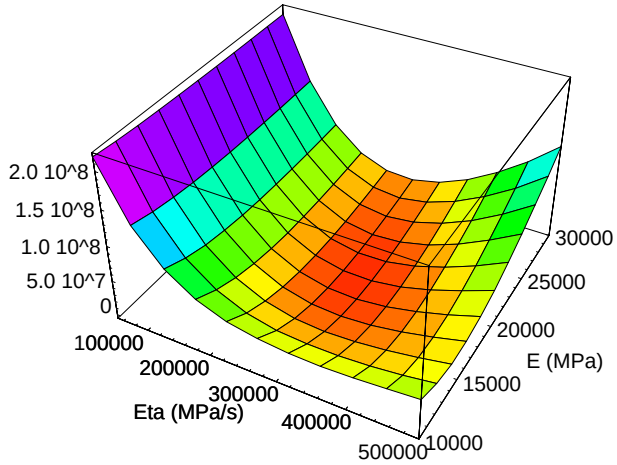

Figure 4. 3D PLOT OF THE COST FUNCTIONAL J

Table 1. IDENTIFICATION RESULTS WITH EXACT MEASUREMENTS

(E^{ini}, η^{ini})	$(E^{final}, \eta^{final})$
(MPa, MPa/s)	(MPa, MPa/s)
(4000., 70000.)	(20002., 30004.)
(60000., 10000.)	(20002., 30009.)
(10000., 5000.)	(20002., 30006.)
(60000., 90000.)	(19999., 29999.)

with different starting points but with the same measurement perturbation. The identified values lie at 2.5% from the real values for both measurement perturbations.

The path of the algorithm on the isovalues of the perturbed cost functional is shown on Figure 7.

Figure 8 shows the real indentation curve ($E = 2 \times 10^4$ MPa, $\eta = 3 \times 10^4$ MPa/s) in comparaison to the initial ($E = 6 \times 10^4$ MPa, $\eta = 9 \times 10^4$ MPa/s) and converged ($E = 1.95 \times 10^4$ MPa, $\eta = 2.91 \times 10^4$ MPa/s) indentation curve. In terms of cost functional the algorithm brought its value from $\approx 10^8$ to $\approx 10^4$. This is the minimal value of the cost functional where the algorithm could descent. However, there is a good agreement between the experimental and identified indentation curve.

Uniqueness and Stability

Even if no precise proof of uniqueness and stability has been provided, one can notice that the cost functional is almost convex and presents a unique minimum in the domain of physical interest (Figure 4). For other values of the material parameters $\boldsymbol{c} = (E, \eta)$ we have obtained similar shapes of the cost functional. It is important to state that identifications started with values outside the presented range did also converge to the same parameter pair. All these remarks suggest that this inverse identification problem has a unique solution.

The stability of the inverse problem is revealed by the sensitivity of the identification with regards to measurement noise. The results show that even 10% noise do not affect the identified value by more than 2.5%.

In evaluating the results its is also important to notice that no regularization procedure (Tikhonov or other) has been used during the identification.

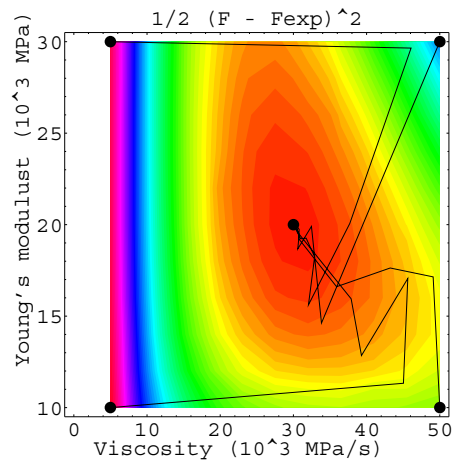

Figure 5. PATH OF THE ALGORITHM (exact measurements)

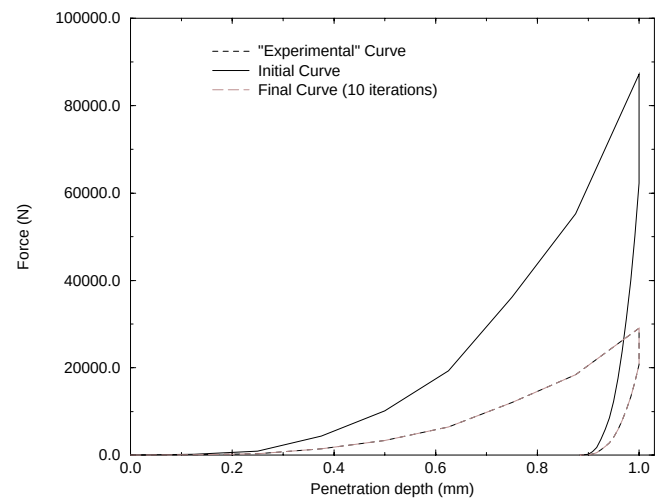

Figure 6. EVOLUTION OF THE INDENTATION CURVE WITH EXACT MEASUREMENTS

Copyright © 1999 by ASME

Table 2. IDENTIFICATION RESULTS FROM MEASUREMENTS WITH RANDOM ERROR

(E^{ini}, η^{ini}) (MPa, MPa/s)	$(E^{final}, \eta^{final})$ (MPa, MPa/s)
(4000., 70000.)	(20580., 30490.)
(10000., 5000.)	(20611., 30457.)
(60000., 10000.)	(19509., 29130.)
(60000., 90000.)	(19509., 29136.)

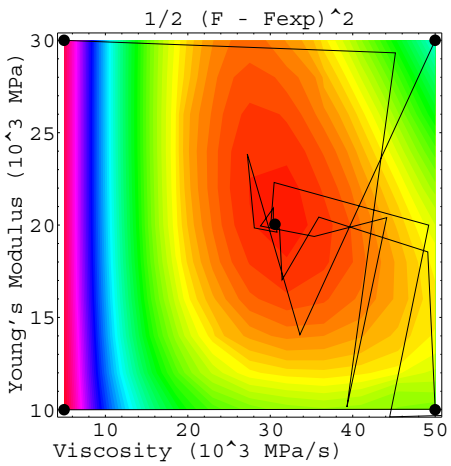

Figure 7. PATH OF THE ALGORITHM (measurements with random error)

CONCLUSION

The identification of the parameters of a standard generalized non hardening constitutive law from indentation tests was presented. It has been shown that the adjoint state method can be extended to contact problems using Lagrange multipliers.

The efficiency of the method has been illustrated on a numerical example for an indentation problem in the case of a Maxwell viscoelatic problem. The numerical results suggest the well-posedness (existence, uniqueness and stability of the solution) for this inverse problem. The precise proof of this result is still an open question.

The method is extendable to other types of material behaviour or loading conditions.

ACKNOWLEDGMENT

The authors would like to thank Said Taheri, Stéphane Andrieux and Laurent Bourgeois for helpfull discussions and Marc Bonnet for reading this paper. They would also like to acknowledge the financial support of EDF - Electricité de France for this work.

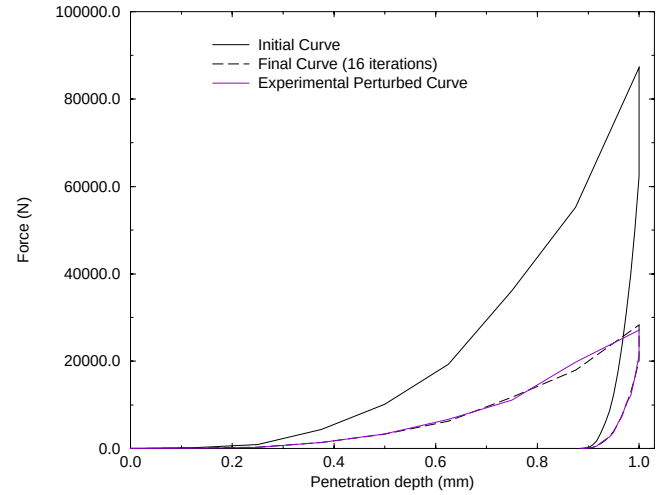

Figure 8. EVOLUTION OF THE INDENTATION CURVE FROM MEASUREMENTS WITH RANDOM ERROR

REFERENCES

L. Bourgeois, *Contrôle optimal et problèmes inverses en plasticité*, Ph.D. thesis, École Polytechnique, 1998.

H.D. Bui, *Inverse problems in the mechanics of materials : an introduction*, CRC Press, Boca Raton, 1994.

A. Constantinescu, N. Tardieu, *The adjoint state method applied to material identification through indentation tests*, Advances in Finite Element Procedures and Techniques, Civil Comp Press, 1998.

P.E. Gill, W. Murray, M.H. Wright, *Practical optimization*, Academic Press, 1981.

B. Halphen, Q.S. Nguyen, *Sur les matériaux standards généralisés*, Journal de Mécanique, 1975.

A. Hasanov, Z. Seyidmamedov, *The solution of an axisymetric inverse elastoplastic problem using penetration diagrams*, Int. J. Non-Linear Mech., Vol. 30, 1995.

S. Jayaraman, G.T. Hahn, W.C. Oliver, C.A. Rubin, P.C. Bastias, *Determination of monotonic stress-strain curve of hard metals from ultra-low-load indentation tests*, Int. J. Solids Structures, Vol. 35, Nos. 5-6, 1998.

K.L. Johnson, *Contact mechanics*, Cambridge University Press, 1985.

N. Kikuchi, J.T. Oden, *Contact problems in elasticity : a study of variational inequalities and finite element methods*, SIAM, Philadelphia, 1988.

J.L. Lions, *Contrôle optimal des systèmes gouvernés par des équations aux dérivées partielles*, Dunod, 1968.

B. Taljat, T. Zacharia, F. Kosel *New analytical procedure to determine stress-strain curve from spherical indentation data*, Int. J. Solids Structures, Vol. 35, No. 33, 1998.

Copyright © 1999 by ASME